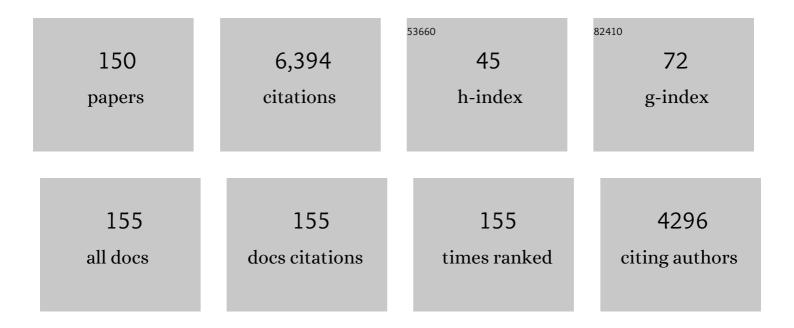
List of Publications by Year in descending order

Source: https://exaly.com/author-pdf/2156992/publications.pdf Version: 2024-02-01



#	Article	IF	CITATIONS
1	Sr-Nd-Pb composition of Mesozoic Pacific oceanic crust (Site 1149 and 801, ODP Leg 185): Implications for alteration of ocean crust and the input into the Izu-Bonin-Mariana subduction system. Geochemistry, Geophysics, Geosystems, 2003, 4, .	1.0	206
2	Arc-parallel flow in the mantle wedge beneath Costa Rica and Nicaragua. Nature, 2008, 451, 1094-1097.	13.7	201
3	Missing history (16–71 Ma) of the Galápagos hotspot: Implications for the tectonic and biological evolution of the Americas. Geology, 2002, 30, 795.	2.0	178
4	Cenozoic intraplate volcanism on New Zealand: Upwelling induced by lithospheric removal. Earth and Planetary Science Letters, 2006, 248, 350-367.	1.8	172
5	Combined Trace Element and Pb-Nd-Sr-O Isotope Evidence for Recycled Oceanic Crust (Upper and) Tj ETQq1 1 0	0.784314 i 1.1	∙gB <u>T</u> /Qverlac
6	Age and geochemistry of basaltic complexes in western Costa Rica: Contributions to the geotectonic evolution of Central America. Geochemistry, Geophysics, Geosystems, 2000, 1, .	1.0	152
7	Large volume recycling of oceanic lithosphere over short time scales: geochemical constraints from the Caribbean Large Igneous Province. Earth and Planetary Science Letters, 2000, 174, 247-263.	1.8	140
8	Age and geochemistry of volcanic rocks from the Hikurangi and Manihiki oceanic Plateaus. Geochimica Et Cosmochimica Acta, 2010, 74, 7196-7219.	1.6	140
9	70 m.y. history (139–69 Ma) for the Caribbean large igneous province. Geology, 2004, 32, 697.	2.0	138
10	Temporal and geochemical evolution of the Cenozoic intraplate volcanism of Zealandia. Earth-Science Reviews, 2010, 98, 38-64.	4.0	129
11	Flow of Canary mantle plume material through a subcontinental lithospheric corridor beneath Africa to the Mediterranean. Geology, 2009, 37, 283-286.	2.0	123
12	Plume–subduction interaction in southern Central America: Mantle upwelling and slab melting. Lithos, 2011, 121, 117-134.	0.6	116
13	How and when plume zonation appeared during the 132 Myr evolution of the Tristan Hotspot. Nature Communications, 2015, 6, 7799.	5.8	116
14	Geodynamic evolution of the Galápagos hot spot system (Central East Pacific) over the past 20 m.y.: Constraints from morphology, geochemistry, and magnetic anomalies. Geochemistry, Geophysics, Geosystems, 2003, 4, .	1.0	109
15	Across-arc geochemical variations in the Southern Volcanic Zone, Chile (34.5–38.0°S): Constraints on mantle wedge and slab input compositions. Geochimica Et Cosmochimica Acta, 2013, 123, 218-243.	1.6	105
16	Enriched, HIMU-type peridotite and depleted recycled pyroxenite in the Canary plume: A mixed-up mantle. Earth and Planetary Science Letters, 2009, 277, 514-524.	1.8	104
17	Calcium Isotopes (l̃´ ^{44/40} Ca) in MPIâ€DING Reference Glasses, USGS Rock Powders and Various Rocks: Evidence for Ca Isotope Fractionation in Terrestrial Silicates. Geostandards and Geoanalytical Research, 2009, 33, 231-247.	1.7	103
18	Major, trace element and Nd–Sr–Pb–O–He–Ar isotope signatures of shield stage lavas from the central and western Canary Islands: Insights into mantle and crustal processes. Chemical Geology, 2006, 233, 75-112.	1.4	101

#	Article	IF	CITATIONS
19	Origin of Indian Ocean Seamount Province by shallow recycling of continental lithosphere. Nature Geoscience, 2011, 4, 883-887.	5.4	99
20	Age and geochemistry of the oceanic Manihiki Plateau, SW Pacific: New evidence for a plume origin. Earth and Planetary Science Letters, 2011, 304, 135-146.	1.8	99
21	Evidence for an age progression along the Tristan-Gough volcanic track from new 40Ar/39Ar ages on phenocryst phases. Tectonophysics, 2013, 604, 60-71.	0.9	96
22	Geochemical zonation of the Miocene Alborán Basin volcanism (westernmost Mediterranean): geodynamic implications. Contributions To Mineralogy and Petrology, 2008, 156, 577-593.	1.2	95
23	Galapagosâ€OIB signature in southern Central America: Mantle refertilization by arc–hot spot interaction. Geochemistry, Geophysics, Geosystems, 2009, 10, .	1.0	94
24	Continental crust generated in oceanic arcs. Nature Geoscience, 2015, 8, 321-327.	5.4	94
25	Calcium isotope (δ44/40Ca) fractionation along hydrothermal pathways, Logatchev field (Mid-Atlantic) Tj ETQq1	1 0.7843 1.6	14 rgBT /Ove
26	Basalts erupted along the Tongan fore arc during subduction initiation: Evidence from geochronology of dredged rocks from the Tonga fore arc and trench. Geochemistry, Geophysics, Geosystems, 2012, 13, .	1.0	85
27	A Mid Cretaceous origin for the Galápagos hotspot: volcanological, petrological and geochemical evidence from Costa Rican oceanic crustal segments. Geologische Rundschau: Zeitschrift Fur Allgemeine Geologie, 1997, 86, 141-155.	1.3	82
28	New constraints on the age and evolution of the Wishbone Ridge, southwest Pacific Cretaceous microplates, and Zealandia–West Antarctica breakup. Geology, 2006, 34, 185.	2.0	82
29	Transition from arc to oceanic magmatism at the Kamchatka-Aleutian junction. Geology, 2005, 33, 25.	2.0	81
30	On- and off-axis chemical heterogeneities along the South Atlantic Mid-Ocean-Ridge (5–11°S): Shallow or deep recycling of ocean crust and/or intraplate volcanism?. Earth and Planetary Science Letters, 2011, 306, 86-97.	1.8	80
31	Magma genesis by rifting of oceanic lithosphere above anomalous mantle: Terceira Rift, Azores. Geochemistry, Geophysics, Geosystems, 2008, 9, .	1.0	78
32	70 Ma chemical zonation of the Tristan-Gough hotspot track. Geology, 2013, 41, 335-338.	2.0	72
33	A stable (Li, O) and radiogenic (Sr, Nd) isotope perspective on metasomatic processes in a subducting slab. Chemical Geology, 2011, 281, 151-166.	1.4	70
34	Magma storage and ascent during the 1995 eruption of Fogo, Cape Verde Archipelago. Contributions To Mineralogy and Petrology, 2011, 162, 751-772.	1.2	70
35	Osbourn Trough: Structure, geochemistry and implications of a mid-Cretaceous paleospreading ridge in the South Pacific. Earth and Planetary Science Letters, 2006, 245, 685-701.	1.8	64
36	Tracing the effects of high-pressure metasomatic fluids and seawater alteration in blueschist-facies overprinted eclogites: Implications for subduction channel processes. Chemical Geology, 2012, 292-293, 69-87.	1.4	64

FOLKMAR HAUFF

possignetal vocume rocks, Larkin and Panetary Science Letters, 2003, 214, 107-160. 38 Age and Geochemistry of the Central American Forearc Basement (DSDP Leg 67 and 84): Insights into 1.1 53 39 Mesociok Arv Volcanism and Seamount Accretion on the Fringe of the Carlbban UP. Journal of Petrology, 2008, 49, 1781-1815. 0.8 53 39 Tecedemistry of the late Holocene rocks from the Tolbachik volcanic field, Kamchatka: Quantitative magnatic systems, Journal of Volcanology and Geothermal Research, 2015, 307, 133-155. 0.8 53 40 Hafnium isotopic variations in volcanic rocks from the Carlbbaen Large igneous Province and CalApagos hot spot tracks. Geochemistry, Geophysics, Geosystems, 2003, 4, . 1.0 52 41 Olivine Major and Trace Element Compositions in Southern Agentia Basalis, Argentina: Evidence for Pyroxenites/Crendotite Melt Mixing in a Back-arc Setting, Journal of Petrology, 2015, 56, 1495-1518. 1.1 51 42 Geochemical approaches to the quantification of dispersed volcanic ash in marine sediment. Progress 1.1 51 43 Inplications for a Common Source for the Emazert and Canary and Cape Verde Island Carbonattes. 1.1 50 44 Subduction initiation terranse exposed at the front of a 2 Ma volcanically-active subduction zone. 1.8 49 45 Earth and Planetary Science Laters, 2019, 508, 30-40. 1.0 48	¥	Article	IF	CITATIONS
38 Mesozole Arc Volcanism and Seamount Accretion on the Fringe of the Carlbbean LIP. Journal of 1.1 53 39 Petrology, 2008, 49, 1781-1815. 0.8 53 30 Geochemistry of the late Holocene rocks from the Tolbachik volcanic field, Kamchatka: Quantitative modelling of subduction-related open magmatic systems. Journal of Volcanology and Geothermal Research, 2015, 307, 133-155. 0.8 53 40 Hafnium Isotopic variations in volcanic rocks from the Carlbbean Large Igneous Province and GalAipagos hot spot tracks. Geochemistry, Geophysics, Geosystems, 2003, 4, . 1.0 52 41 Olivine Major and Trace Element Compositions in Southern Payenia Basalts, Argentina: Evidence for Pyroxenite3e: Periodotic Melt Mixing in a Back arc Setting. Journal of Petrology, 2015, 56, 1495-1518. 1.1 61 42 Geochemical approaches to the quantification of dispersed volcanic ash in marine sediment. Progress in Earth and Planetary Science, 2016, 3, . 1.1 61 43 Petrogenesis of the Eocene Tamazert Continental Carbonatites (Central High Atlas, Morocco): Implications for a Common Source for the Tamazert and Canary and Cape Verde Island Carbonatites. 1.1 62 44 Euchemical approaches to the quantification of a 2 Ma volcanically-active subduction zone. 1.8 49 45 Subduction Initiation terranes exposed at the front of a 2 Ma volcanically-active subduction zone. 1.8 49	37		1.8	63
39 modelling of subduction related open magmatic systems. Journal of Volcanology and Geothermal Research, 2015, 307, 133-155. 0.8 53 40 Hafnium isotopic variations in volcanic rocks from the Caribbean Large Igneous Province and Galkipages hot spot tracks. Geochemistry, Geophysics, Geosystems, 2003, 4,. 1.0 52 41 Polvine Major and Trace Element Compositions in Southern Payenia Basalts, Argentina: Evidence for Pyroxenite&C*Peridotte Melt Muking in a Backarc Setting. Journal of Petrology, 2015, 56, 1495-1518. 1.1 51 42 Geochemical approaches to the quantification of dispersed volcanic ash in marine sediment. Progress in Earth and Planetary Science, 2016, 3, . 1.1 51 43 Inplications for a Common Source for the Tamazert and Canary and Cape Verde Island Carbonatites. 1.1 56 44 Eutrology, 2010, 51, 1655-1686. 1.1 56 46 45 Subduction Initiation terranes exposed at the front of a 2 Ma volcanically-active subduction zone. 1.8 49 46 Mid Cretaceous Hawalian tholelites preserved in Kamchatka. Geology, 2008, 36, 903. 2.0 48 47 Source components of the Gran Canaria (Canary Islands) shield stage magmas: evidence from olivine composition and Srae*Ndae*Pb isotopes. Contributions To Mineralogy and Petrology, 2010, 159, 689-702. 1.2 47 48 Plumeäd*ridge Interaction studied a	38	Mesozoic Arc Volcanism and Seamount Accretion on the Fringe of the Caribbean LIP. Journal of	1.1	53
40 GalÄppagos höt spot tracks. Geochemistry, Geophysics, Geosystems, 2003, 4, . 1.0 32 41 Olivine Major and Trace Element Compositions in Southern Payenia Basahs, Argentina: Evidence for PyroxeniteåC"Peridotite Melk Mixing in a Back-arc Setting, Journal of Petrology, 2015, 56, 1495-1518. 1.1 51 42 Geochemical approaches to the quantification of dispersed volcanic ash in marine sediment. Progress 1.1 51 43 In Earth and Planetary Science, 2016, 3, . 1.1 51 44 Subduction for a Common Source for the Tamazert and Canary and Cape Verde Island Carbonatites. 1.1 56 44 Subduction initiation terranes exposed at the front of a 2 Ma volcanically-active subduction zone. 1.8 49 45 Morphological and geochemical variations along the eastern CalÄpagos Spreading Center. 1.0 48 46 Mid-Cretaceous Hawaiian tholeiites preserved in Kamchatka. Geology, 2008, 36, 903. 2.0 48 47 Source components of the Cran Canaria (Canary Islands) shield stage magmas: evidence from olivine composition and Srae"Nd&CPb Isotopes. Contributions To Mineralogy and Petrology, 2010, 159, 689-702. 1.2 47 48 Plumeå@"irdge interaction studied at the CalÄpagos spreading center: Evidence from 226Raa@"230Tha@"238U and 231Paa&"235U Isotopic disequilibria. Earth and Planetary Science Letters, 2005, 234, 165-187. <	39	modelling of subduction-related open magmatic systems. Journal of Volcanology and Geothermal	0.8	53
PyroxeniteãC*Peridotite Melt Mixing in a Back-arc Setting, Journal of Petrology, 2015, 56, 1495-1518. In In 42 Geochemical approaches to the quantification of dispersed volcanic ash in marine sediment. Progress in Earth and Planetary Science, 2016, 3, . 1.1 51 43 Petrogenesis of the Eocene Tamazert Continental Carbonatites (Central High Atlas, Morocco): Implications for a Common Source for the Tamazert and Canary and Cape Verde Island Carbonatites. 1.1 50 44 Subduction Initiation terranes exposed at the front of a 2 Ma volcanically-active subduction zone. 1.8 49 45 Morphological and geochemical variations along the eastern GalAipagos Spreading Center. 1.0 48 46 Mid-Cretaceous Hawaiian tholeiltes preserved in Kamchatka. Geology, 2008, 36, 903. 2.0 48 47 Source components of the Gran Canaria (Canary Islands) shield stage magmas: evidence from olivine composition and SraC'NdaC'Pb isotopes. Contributions To Mineralogy and Petrology, 2010, 159, 689-702. 1.2 47 48 PlumeáC**ridge interaction studied at the GalAipagos spreading center: Evidence from olivine composition of the oceanic Hikurangi Plateau and its impact on the Kermadec arc. Nature Communications, 2014, 5, 4923. 5.8 45 50 Melts of sediments in the mantle wedge of the Oman ophiolite. Geology, 2015, 43, 275-278. 2.0 45 50 Melts of	40		1.0	52
14 in Earth and Planetary Science, 2016, 3, . 11 51 14 Petrogenesis of the Eocene Tamazert Continental Carbonatites (Central High Atlas, Morocco): Implications for a Common Source for the Tamazert and Canary and Cape Verde Island Carbonatites. Journal of Petrology, 2010, 51, 1655-1686. 11 50 14 Subduction initiation terranes exposed at the front of a 2 Ma volcanically-active subduction zone. Earth and Planetary Science Letters, 2019, 508, 30-40. 1.8 49 45 Morphological and geochemical variations along the eastern CalAipagos Spreading Center. Geochemistry, Geophysics, Geosystems, 2005, 6, n/a-n/a. 1.0 48 46 Mid-Cretaceous Hawaiian tholeiites preserved in Kamchatka. Geology, 2008, 36, 903. 2.0 48 47 Source components of the Gran Canaria (Canary Islands) shield stage magmas: evidence from olivine composition and Srāć "Ndãć"Pb isotopes. Contributions To Mineralogy and Petrology, 2010, 159, 689-702. 1.2 47 48 Plumeãé "ridge interaction studied at the CalAipagos spreading center: Evidence from 226Raãć "230Thãć" 238U and 231Paãé" 235U isotopic disequilibria. Earth and Planetary Science Letters, 2005, 234, 165-187. 1.8 45 49 Subduction of the oceanic Hikurangi Plateau and its impact on the Kermadec arc. Nature Communications, 2014, 5, 4923. 5.8 45 50 Melts of sediments in the mantle wedge of the Oman ophiolite. Geology, 2015, 43, 275-278.	41	Olivine Major and Trace Element Compositions in Southern Payenia Basalts, Argentina: Evidence for Pyroxenite–Peridotite Melt Mixing in a Back-arc Setting. Journal of Petrology, 2015, 56, 1495-1518.	1.1	51
43 Implications for a Common Source for the Tamazert and Canary and Cape Verde Island Carbonatites. 1.1 50 44 Subduction Initiation terranes exposed at the front of a 2 Ma volcanically-active subduction zone. 1.8 49 44 Subduction Initiation terranes exposed at the front of a 2 Ma volcanically-active subduction zone. 1.8 49 45 Morphological and geochemical variations along the eastern GalÅ;pagos Spreading Center. 1.0 48 46 Mid-Cretaceous Hawaiian tholeiites preserved in Kamchatka. Geology, 2008, 36, 903. 2.0 48 47 Source components of the Cran Canaria (Canary Islands) shield stage magmas: evidence from olivine composition and Srå€"Nda€"Pb isotopes. Contributions To Mineralogy and Petrology, 2010, 159, 689-702. 1.2 47 48 Plumeå€"ridge interaction studied at the GalÅ;pagos spreading center: Evidence from 226Raå€"230Thâ€"238U 1.8 45 49 Subduction of the oceanic Hikurangi Plateau and its impact on the Kermadec arc. Nature Communications, 2014, 5, 4923. 5.8 45 50 Melts of sediments in the mantle wedge of the Oman ophiolite. Geology, 2015, 43, 275-278. 2.0 45 50 Melts of sediments in the mattle wedge of the Oman ophiolite. Geology, 2015, 43, 275-278. 2.0 45 50 Melts of sediments in the mattle wedge	12	Geochemical approaches to the quantification of dispersed volcanic ash in marine sediment. Progress in Earth and Planetary Science, 2016, 3, .	1.1	51
44 Earth and Planetary Science Letters, 2019, 508, 30-40. 1.8 49 45 Morphological and geochemical variations along the eastern GalÄipagos Spreading Center. Ceochemistry, Geophysics, Geosystems, 2005, 6, n/a-n/a. 1.0 48 46 Mid-Cretaceous Hawaiian tholeiites preserved in Kamchatka. Geology, 2008, 36, 903. 2.0 48 47 Source components of the Gran Canaria (Canary Islands) shield stage magmas: evidence from olivine composition and Sr–Nd–Pb isotopes. Contributions To Mineralogy and Petrology, 2010, 159, 689-702. 1.2 47 48 Plume–ridge interaction studied at the GalÃipagos spreading center: Evidence from 226Ra–230Th–238U and 231Pa—235U isotopic disequilibria. Earth and Planetary Science Letters, 2005, 234, 165-187. 1.8 45 49 Subduction of the oceanic Hikurangi Plateau and its impact on the Kermadec arc. Nature Communications, 2014, 5, 4923. 5.8 45 50 Melts of sediments in the mantle wedge of the Oman ophiolite. Geology, 2015, 43, 275-278. 2.0 45 50 Melts of sediments in the mantle wedge of the Oman ophiolite. Geology, 2015, 43, 275-278. 2.0 45 50 Melts of sediments in the mantle wedge of the Oman ophiolite. Geology, 2015, 43, 275-278. 2.0 45	13	Implications for a Common Source for the Tamazert and Canary and Cape Verde Island Carbonatites.	1.1	50
 Geochemistry, Geophysics, Geosystems, 2005, 6, n/a-n/a. Mid-Cretaceous Hawaiian tholeiites preserved in Kamchatka. Geology, 2008, 36, 903. Source components of the Gran Canaria (Canary Islands) shield stage magmas: evidence from olivine composition and Sr–Nd–Pb isotopes. Contributions To Mineralogy and Petrology, 2010, 159, 689-702. Plume–ridge interaction studied at the GalÃipagos spreading center: Evidence from 226Ra–230Th–238U and 231Pa–235U isotopic disequilibria. Earth and Planetary Science Letters, 2005, 234, 165-187. Subduction of the oceanic Hikurangi Plateau and its impact on the Kermadec arc. Nature Communications, 2014, 5, 4923. Melts of sediments in the mantle wedge of the Oman ophiolite. Geology, 2015, 43, 275-278. Continuation of the New England Orogen, Australia, beneath the Queensland Plateau and Lord Howe 	14		1.8	49
 Source components of the Gran Canaria (Canary Islands) shield stage magmas: evidence from olivine composition and Sr–Nd–Pb isotopes. Contributions To Mineralogy and Petrology, 2010, 159, 689-702. Plume–ridge interaction studied at the GalÃipagos spreading center: Evidence from 226Ra–230Th–238U and 231Pa—235U isotopic disequilibria. Earth and Planetary Science Letters, 2005, 234, 165-187. Subduction of the oceanic Hikurangi Plateau and its impact on the Kermadec arc. Nature 5.8 45 Melts of sediments in the mantle wedge of the Oman ophiolite. Geology, 2015, 43, 275-278. Continuation of the New England Orogen, Australia, beneath the Queensland Plateau and Lord Howe 0.4 45 	15		1.0	48
 composition and Sr–Nd–Pb isotopes. Contributions To Mineralogy and Petrology, 2010, 159, 689-702. Plume–ridge interaction studied at the Galápagos spreading center: Evidence from 226Ra–230Th–238U and 231Pa–235U isotopic disequilibria. Earth and Planetary Science Letters, 2005, 234, 165-187. Subduction of the oceanic Hikurangi Plateau and its impact on the Kermadec arc. Nature 5.8 Subductions, 2014, 5, 4923. Melts of sediments in the mantle wedge of the Oman ophiolite. Geology, 2015, 43, 275-278. Continuation of the New England Orogen, Australia, beneath the Queensland Plateau and Lord Howe 	16	Mid-Cretaceous Hawaiian tholeiites preserved in Kamchatka. Geology, 2008, 36, 903.	2.0	48
 Subduction of the oceanic Hikurangi Plateau and its impact on the Kermadec arc. Nature Communications, 2014, 5, 4923. Melts of sediments in the mantle wedge of the Oman ophiolite. Geology, 2015, 43, 275-278. Continuation of the New England Orogen, Australia, beneath the Queensland Plateau and Lord Howe 	17	Source components of the Gran Canaria (Canary Islands) shield stage magmas: evidence from olivine composition and Sr–Nd–Pb isotopes. Contributions To Mineralogy and Petrology, 2010, 159, 689-702.	1.2	47
 Communications, 2014, 5, 4923. Melts of sediments in the mantle wedge of the Oman ophiolite. Geology, 2015, 43, 275-278. Continuation of the New England Orogen, Australia, beneath the Queensland Plateau and Lord Howe 	18	Plume–ridge interaction studied at the Galápagos spreading center: Evidence from 226Ra–230Th–238U and 231Pa–235U isotopic disequilibria. Earth and Planetary Science Letters, 2005, 234, 165-187.	1.8	45
Continuation of the New England Orogen, Australia, beneath the Queensland Plateau and Lord Howe	19	Subduction of the oceanic Hikurangi Plateau and its impact on the Kermadec arc. Nature Communications, 2014, 5, 4923.	5.8	45
	50	Melts of sediments in the mantle wedge of the Oman ophiolite. Geology, 2015, 43, 275-278.	2.0	45
Rise. Australian Journal of Earth Sciences, 2008, 55, 195-209.	51	Continuation of the New England Orogen, Australia, beneath the Queensland Plateau and Lord Howe Rise. Australian Journal of Earth Sciences, 2008, 55, 195-209.	0.4	40
52Global distribution of the HIMU end member: Formation through Archean plume-lid tectonics.4.04052Earth-Science Reviews, 2018, 182, 85-101.4.040	52	Global distribution of the HIMU end member: Formation through Archean plume-lid tectonics. Earth-Science Reviews, 2018, 182, 85-101.	4.0	40
New age and geochemical data from the Walvis Ridge: The temporal and spatial diversity of South 53 Atlantic intraplate volcanism and its possible origin. Geochimica Et Cosmochimica Acta, 2019, 245, 1.6 40 16-34.	53	Atlantic intraplate volcanism and its possible origin. Geochimica Et Cosmochimica Acta, 2019, 245,	1.6	40

54 Hydrothermal activity and magma genesis along a propagating back-arc basin: Valu Fa Ridge (southern) Tj ETQq0 0.0 rgBT /Oyerlock 10

#	Article	IF	CITATIONS
55	Along and across arc geochemical variations in NW Central America: Evidence for involvement of lithospheric pyroxenite. Geochimica Et Cosmochimica Acta, 2012, 84, 459-491.	1.6	39
56	Seamounts off the West Antarctic margin: A case for non-hotspot driven intraplate volcanism. Gondwana Research, 2014, 25, 1660-1679.	3.0	38
57	Deformation-related volcanism in the Pacific Ocean linked to the Hawaiian–Emperor bend. Nature Geoscience, 2015, 8, 393-397.	5.4	38
58	Constraints on the magmatic evolution of the oceanic crust from plagiogranite intrusions in the Oman ophiolite. Contributions To Mineralogy and Petrology, 2016, 171, 1.	1.2	37
59	Boninite-like intraplate magmas from Manihiki Plateau require ultra-depleted and enriched source components. Nature Communications, 2017, 8, 14322.	5.8	37
60	Geochemistry of primitive lavas of the Central Kamchatka Depression: Magma generation at the edge of the Pacific Plate. Geophysical Monograph Series, 2007, , 199-239.	0.1	36
61	Regionalâ€scale input of dispersed and discrete volcanic ash to the <scp>I</scp> zuâ€ <scp>B</scp> onin and <scp>M</scp> ariana subduction zones. Geochemistry, Geophysics, Geosystems, 2014, 15, 4369-4379.	1.0	35
62	Time-scales for magmatic differentiation at the Snaefellsjökull central volcano, western Iceland: Constraints from U–Th–Pa–Ra disequilibria in post-glacial lavas. Geochimica Et Cosmochimica Acta, 2009, 73, 1120-1144.	1.6	34
63	Missing western half of the <scp>P</scp> acific <scp>P</scp> late: Geochemical nature of the <scp>I</scp> zanagiâ€ <scp>P</scp> acific <scp>R</scp> idge interaction with a stationary boundary between the <scp>I</scp> ndian and <scp>P</scp> acific mantles. Geochemistry, Geophysics, Geosystems, 2015, 16, 3309-3332.	1.0	34
64	Origin of enriched components in the South Atlantic: Evidence from 40 Ma geochemical zonation of the Discovery Seamounts. Earth and Planetary Science Letters, 2016, 441, 167-177.	1.8	34
65	Unexpected HIMU-type late-stage volcanism on the Walvis Ridge. Earth and Planetary Science Letters, 2018, 492, 251-263.	1.8	34
66	Mineralogy, geochemistry and stratigraphy of the Maslovsky Pt–Cu–Ni sulfide deposit, Noril'sk Region, Russia. Mineralium Deposita, 2012, 47, 69-88.	1.7	33
67	Magmatic evolution of a dying spreading axis: Evidence for the interaction of tectonics and mantle heterogeneity from the fossil Phoenix Ridge, Drake Passage. Chemical Geology, 2011, 280, 115-125.	1.4	31
68	Bowers Ridge (Bering Sea): An Oligocene-Early Miocene island arc. Geology, 2012, 40, 687-690.	2.0	29
69	Petrogenesis of synorogenic high-temperature leucogranites (Damara orogen, Namibia): Constraints from U–Pb monazite ages and Nd, Sr and Pb isotopes. Gondwana Research, 2014, 25, 1614-1626.	3.0	29
70	Tectonic dissection and displacement of parts of Shona hotspot volcano 3500 km along the Agulhas-Falkland Fracture Zone. Geology, 2016, 44, 263-266.	2.0	29
71	Immiscible sulfide melts in primitive oceanic magmas: Evidence and implications from picrite lavas (Eastern Kamchatka, Russia). American Mineralogist, 2018, 103, 886-898.	0.9	29
72	Hafnium isotopic variations in East Atlantic intraplate volcanism. Contributions To Mineralogy and Petrology, 2011, 162, 21-36.	1.2	28

#	Article	IF	CITATIONS
73	Cretaceous fore-arc basalts from the Tonga arc: Geochemistry and implications for the tectonic history of the SW Pacific. Tectonophysics, 2014, 630, 21-32.	0.9	28
74	Geochemistry and age of Shatsky, Hess, and Ojin Rise seamounts: Implications for a connection between the Shatsky and Hess Rises. Geochimica Et Cosmochimica Acta, 2016, 185, 302-327.	1.6	28
75	Syn-orogenic high-temperature crustal melting: Geochronological and Nd–Sr–Pb isotope constraints from basement-derived granites (Central Damara Orogen, Namibia). Lithos, 2014, 192-195, 21-38.	0.6	26
76	Petrogenesis of synorogenic diorite–granodiorite–granite complexes in the Damara Belt, Namibia: Constraints from U–Pb zircon ages and Sr–Nd–Pb isotopes. Journal of African Earth Sciences, 2015, 101, 253-265.	0.9	26
77	Nature and origin of the Mozambique Ridge, SW Indian Ocean. Chemical Geology, 2019, 507, 9-22.	1.4	26
78	Late Cretaceous (99-69 Ma) basaltic intraplate volcanism on and around Zealandia: Tracing upper mantle geodynamics from Hikurangi Plateau collision to Gondwana breakup and beyond. Earth and Planetary Science Letters, 2020, 529, 115864.	1.8	26
79	Paired EMI-HIMU hotspots in the South Atlantic—Starting plume heads trigger compositionally distinct secondary plumes?. Science Advances, 2020, 6, eaba0282.	4.7	26
80	Holocene fluid venting at an extinct Cretaceous seamount, Canary archipelago. Geology, 2011, 39, 855-858.	2.0	25
81	Origin of Meso-Proterozoic post-collisional leucogranite suites (Kaokoveld, Namibia): constraints from geochronology and Nd, Sr, Hf, and Pb isotopes. Contributions To Mineralogy and Petrology, 2012, 163, 1-17.	1.2	25
82	Age and geochemistry of the Beata Ridge: Primary formation during the main phase (~89†Ma) of the Caribbean Large Igneous Province. Lithos, 2019, 328-329, 69-87.	0.6	25
83	Petrogenesis of rift-related tephrites, phonolites and trachytes (Central European Volcanic Province,) Tj ETQq1	1 0.78431 1.4	4 rgBT /Over
84	Geochemical and Volcanological Evolution of La Palma, Canary Islands. Journal of Petrology, 2017, 58, 1227-1248.	1.1	24
85	Influence of the Galapagos hotspot on the East Pacific Rise during Miocene superfast spreading. Geology, 2013, 41, 183-186.	2.0	23
86	Evidence from accreted seamounts for a depleted component in the early Galapagos plume. Geology, 2016, 44, 383-386.	2.0	23
87	New insights into the origin and evolution of the Hikurangi oceanic plateau. Eos, 2004, 85, 401.	0.1	22
88	Basanite to phonolite differentiation within 1550–1750 yr: U-Th-Ra isotopic evidence from the A.D. 1585 eruption on La Palma, Canary Islands. Geology, 2005, 33, 897.	2.0	22
89	Geochronology, geochemistry and Nd, Sr and Pb isotopes of syn-orogenic granodiorites and granites (Damara orogen, Namibia) — Arc-related plutonism or melting of mafic crustal sources?. Lithos, 2014, 200-201, 386-401.	0.6	22
90	Comparing the nature of the western and eastern Azores mantle. Geochimica Et Cosmochimica Acta, 2016, 172, 76-92.	1.6	21

FOLKMAR HAUFF

#	Article	IF	CITATIONS
91	Granitoids and dykes of the Pine Island Bay region, West Antarctica. Antarctic Science, 2012, 24, 473-484.	0.5	20
92	Boron isotope geochemistry and U–Pb systematics of altered MORB from the Australian Antarctic Discordance (ODP Leg 187). Chemical Geology, 2007, 242, 455-469.	1.4	18
93	Generation of magnesian, high-K alkali-calcic granites and granodiorites from amphibolitic continental crust in the Damara orogen, Namibia. Lithos, 2014, 198-199, 217-233.	0.6	18
94	Geochemistry of deep Manihiki Plateau crust: Implications for compositional diversity of large igneous provinces in the Western Pacific and their genetic link. Chemical Geology, 2018, 493, 553-566.	1.4	18
95	Second-stage Caribbean Large Igneous Province volcanism: The depleted Icing on the enriched Cake. Chemical Geology, 2019, 509, 45-63.	1.4	18
96	Geochemical variations in the Cocos Plate subducting beneath Central America: implications for the composition of arc volcanism and the extent of the Galápagos Hotspot influence on the Cocos oceanic crust. International Journal of Earth Sciences, 2009, 98, 901-913.	0.9	17
97	Geochemistry of Etendeka magmatism: Spatial heterogeneity in the Tristan-Gough plume head. Earth and Planetary Science Letters, 2020, 535, 116123.	1.8	17
98	Sr-Nd isotope systematics in 14-28 Ma low-temperature altered mid-ocean ridge basalt from the Australian Antarctic Discordance, Ocean Drilling Program Leg 187. Geochemistry, Geophysics, Geosystems, 2005, 6, n/a-n/a.	1.0	16
99	Paleocene MORB and OIB from the Resolution Ridge, Tasman Sea. Australian Journal of Earth Sciences, 2012, 59, 953-964.	0.4	15
100	From the lavas to the gabbros: 1.25km of geochemical characterization of upper oceanic crust at ODP/IODP Site 1256, eastern equatorial Pacific. Lithos, 2014, 210-211, 289-312.	0.6	15
101	Trench-perpendicular Geochemical Variation Between two Adjacent Kermadec Arc Volcanoes Rumble II East and West: the Role of the Subducted Hikurangi Plateau in Element Recycling in Arc Magmas. Journal of Petrology, 2016, 57, 1335-1360.	1.1	15
102	New Age and Geochemical Data from the Southern Colville and Kermadec Ridges, SW Pacific: Insights into the recent geological history and petrogenesis of the Proto-Kermadec (Vitiaz) Arc. Gondwana Research, 2019, 72, 169-193.	3.0	15
103	Generation of a potassic to ultrapotassic alkaline complex in a syn-collisional setting through flat subduction: Constraints on magma sources and processes (Otjimbingwe alkaline complex, Damara) Tj ETQq1 1 0	.7 &⊕ 314 ı	rg₿₮ /Overlo
104	Silicification of peridotites at the stalemate fracture zone (Northwestern Pacific): Reconstruction of the conditions of low-temperature weathering and tectonic interpretation. Petrology, 2012, 20, 21-39.	0.2	13
105	Extent of the Ross Orogen in Antarctica: new data from DSDP 270 and Iselin Bank. Antarctic Science, 2011, 23, 297-306.	0.5	12
106	Mid-ocean ridge basalt generation along the slow-spreading, South Mid-Atlantic Ridge (5–11°S): Inferences from 238U–230Th–226Ra disequilibria. Geochimica Et Cosmochimica Acta, 2015, 169, 152-166.	1.6	12
107	A 1.5 Ma record of plume-ridge interaction at the Western Galápagos Spreading Center (91°40′–92°00′W). Geochimica Et Cosmochimica Acta, 2016, 185, 141-159.	1.6	12
108	Magmatic Evolution and Source Variations at the Nifonea Ridge (New Hebrides Island Arc). Journal of Petrology, 2017, 58, 473-494.	1.1	12

#	Article	IF	CITATIONS
109	Origin of isolated seamounts in the Canary Basin (East Atlantic): The role of plume material in the origin of seamounts not associated with hotspot tracks. Terra Nova, 2020, 32, 390-398.	0.9	12
110	Ultraâ€fast early Miocene exhumation of Cavalli Seamount, Northland Plateau, Southwest Pacific Ocean. New Zealand Journal of Geology, and Geophysics, 2008, 51, 29-42.	1.0	10
111	Flow of Canary mantle plume material through a subcontinental lithospheric corridor beneath Africa to the Mediterranean: REPLY. Geology, 2010, 38, e203-e203.	2.0	10
112	Basalt Geochemistry and Mantle Flow During Early Backarc Basin Evolution: Havre Trough and Kermadec Arc, Southwest Pacific. Geochemistry, Geophysics, Geosystems, 2021, 22, e2020GC009339.	1.0	10
113	²³⁸ U– ²³⁰ Th– ²²⁶ Ra Disequilibria Constraints on the Magmatic Evolution of the Cumbre Vieja Volcanics on La Palma, Canary Islands. Journal of Petrology, 2015, 56, 1999-2024.	1.1	9
114	Generation of syntectonic calc-alkaline, magnesian granites through remelting of pre-tectonic igneous sources – U-Pb zircon ages and Sr, Nd and Pb isotope data from the Donkerhoek granite (southern Damara orogen, Namibia). Lithos, 2018, 310-311, 314-331.	0.6	9
115	Petrogenesis and Assembly of the Don Manuel Igneous Complex, Miocene–Pliocene Porphyry Copper Belt, Central Chile. Journal of Petrology, 2018, 59, 1067-1108.	1.1	9
116	2.8–1.7ÂGa history of the Jiao-Liao-Ji Belt of the North China Craton from the geochronology and geochemistry of mafic Liaohe meta-igneous rocks. Gondwana Research, 2020, 85, 55-75.	3.0	9
117	Do the 85°E Ridge and Conrad Rise form a hotspot track crossing the Indian Ocean?. Lithos, 2021, 398-399, 106234.	0.6	9
118	Hikurangi Plateau subduction a trigger for Vitiaz arc splitting and Havre Trough opening (southwestern Pacific). Geology, 2021, 49, 536-540.	2.0	9
119	ANATEXIS OF JUVENILE MAFIC TO INTERMEDIATE CRUST -CONSTRAINTS FROM MAJOR AND TRACE ELEMENT AND SR, ND, PB ISOTOPES OF DIORITES TO GRANITES (DAMARA OROGEN, NAMBIA). South African Journal of Geology, 2014, 117, 149-171.	0.6	8
120	Petrogenesis of Tertiary continental intra-plate lavas between Siebengebirge and Westerwald, Germany: Constraints from trace element systematics and Nd, Sr and Pb isotopes. Journal of Volcanology and Geothermal Research, 2015, 305, 84-99.	0.8	8
121	Age and origin of Researcher Ridge and an explanation for the 14° N anomaly on the Mid-Atlantic Ridge by plume-ridge interaction. Lithos, 2019, 326-327, 540-555.	0.6	8
122	Ultraslow Spreading and Volcanism at the Eastern End of Gakkel Ridge, Arctic Ocean. Geochemistry, Geophysics, Geosystems, 2019, 20, 6033-6050.	1.0	7
123	Crust-mantle interaction during syn-collisional magmatism – Evidence from the Oamikaub diorite and Neikhoes metagabbro (Damara orogen, Namibia). Precambrian Research, 2020, 351, 105955.	1.2	7
124	Petrogenesis of the late Paleoproterozoic Gleibat Lafhouda dolomite carbonatite (West African) Tj ETQq0 0 0 rg supercontinent. Chemical Geology, 2022, 594, 120764.	BT /Overlc 1.4	ock 10 Tf 50 1 7
125	Cocos Plate Seamounts offshore NW Costa Rica and SW Nicaragua: Implications for large-scale distribution of Gal¡pagos plume material in the upper mantle. Lithos, 2015, 212-215, 214-230.	0.6	6
126	Contrasting magmatic cannibalism forms evolved phonolitic magmas in the Canary Islands. Geology, 2017, 45, 147-150.	2.0	6

FOLKMAR HAUFF

#	Article	IF	CITATIONS
127	Petrogenesis of basalts along the eastern Woodlark spreading center, equatorial western Pacific. Lithos, 2018, 316-317, 122-136.	0.6	6
128	Gigantic eruption of a Carpathian volcano marks the largest Miocene transgression of Eastern Paratethys. Earth and Planetary Science Letters, 2021, 563, 116890.	1.8	6
129	Papanin Ridge and Ojin Rise Seamounts (Northwest Pacific): Dual Hotspot Tracks Formed by the Shatsky Plume. Geochemistry, Geophysics, Geosystems, 2021, 22, e2021GC009847.	1.0	6
130	New Calcium Carbonate Nanoâ€particulate Pressed Powder Pellet (NFHSâ€2â€NP) for LAâ€ICPâ€OES, LAâ€(MC and µXRF. Geostandards and Geoanalytical Research, 2022, 46, 411-432.	:)â €iC Pâ€i 1.7	MS ₆
131	Composition and timing of carbonate vein precipitation within the igneous basement of the Early Cretaceous Shatsky Rise, NW Pacific. Marine Geology, 2014, 357, 321-333.	0.9	5
132	231Pa systematics in postglacial volcanic rocks from Iceland. Geochimica Et Cosmochimica Acta, 2016, 185, 129-140.	1.6	5
133	Oceanic igneous complexes. , 2007, , .		5
134	Age progressive volcanism opposite Nazca plate motion: Insights from seamounts on the northeastern margin of the Galapagos Platform. Lithos, 2018, 310-311, 342-354.	0.6	4
135	Petrogenesis of shield volcanism from the Juan Fernández Ridge, Southeast Pacific: Melting of a low-temperature pyroxenite-bearing mantle plume. Geochimica Et Cosmochimica Acta, 2019, 257, 311-335.	1.6	4
136	Discovery of Ancient Volcanoes in the Okhotsk Sea (Russia): New Constraints on the Opening History of the Kurile Back Arc Basin. Geosciences (Switzerland), 2020, 10, 442.	1.0	4
137	Petrology and geochemistry of plutonic rocks in the Northwest Pacific Ocean and their geodynamic interpretation. Geochemistry International, 2014, 52, 179-196.	0.2	3
138	Compositional variation and ²²⁶ Raâ€ ²³⁰ Th model ages of axial lavas from the southern Midâ€Atlantic Ridge, 8°48′S. Geochemistry, Geophysics, Geosystems, 2016, 17, 199-218.	1.0	3
139	Sr-Nd-Pb-Hf-O isotopic constraints on the Neoproterozoic to Miocene upper and mid crust in central Chile and western Argentina and trench sediments (33°-35°S). Journal of South American Earth Sciences, 2020, 104, 102879.	0.6	3
140	Petrogenesis of a low-87Sr/86Sr, two-mica, garnet-bearing leucogranite (Donkerhoek batholith,) Tj ETQq0 0 0 rg	BT /Qverlo	ock ₃ 10 Tf 50 2
141	Petrogenesis of a late-stage calc-alkaline granite in a giant S-type batholith: geochronology and Sr–Nd–Pb isotopes from the Nomatsaus granite (Donkerhoek batholith), Namibia. International Journal of Earth Sciences, 2021, 110, 1453-1476.	0.9	3
142	Melting of metasomatically enriched lithospheric mantle – Constraints from Pan-African monzonites (Damara Orogen, Namibia). Lithos, 2021, 398-399, 106332.	0.6	3
143	Hydrothermal versus active margin sediment supply to the eastern equatorial Pacific over the past 23 million years traced by radiogenic Pb isotopes: Paleoceanographic and paleoclimatic implications. Geochimica Et Cosmochimica Acta, 2016, 190, 213-238.	1.6	2
144	Enriched mantle one (EMI) type carbonatitic volcanism in Namibia: Evidence for a concentrically-zoned Etendeka plume head. Gondwana Research, 2022, 109, 239-252.	3.0	2

9

#	Article	IF	CITATIONS
145	A Mid Cretaceous origin for the Galápagos hotspot: volcanological, petrological and geochemical evidence from Costa Rican oceanic crustal segments. , 1997, 86, 141.		1
146	Geochemistry and petrogenesis of alkaline rear-arc magmatism in NW Iran. Lithos, 2022, 412-413, 106590.	0.6	1
147	Mineralogy and geochemistry of lavas from the submarine lower caldera walls of Santorini Volcano (Greece). Journal of Volcanology and Geothermal Research, 2022, 427, 107556.	0.8	1
148	Insights into the petrogenesis of an intraplate volcanic province: Sr-Nd-Pb-Hf isotope geochemistry of the Bathymetrists Seamount Province, eastern equatorial Atlantic. Chemical Geology, 2020, 544, 119599.	1.4	0
149	Shear-assisted water-fluxed melting and AFC processes in the foreland of the EarlyÂPaleozoic Famatinian orogen: petrogenesis of leucogranites and pegmatites from the Sierras de Córdoba, Argentina. International Journal of Earth Sciences, 2021, 110, 2495-2517.	0.9	0
150	40Ar/39Ar ages and bulk-rock chemistry of the lower submarine units of the central and western Aleutian Arc. Lithos, 2021, 392-393, 106147.	0.6	0